JOURNAL OF MATERIALS SCIENCE 35 (2000) 735–746

Dissolution behaviour of stainless steel weld metals during active potential range: A calculational approach

M. G. PUJAR, R. K. DAYAL
Corrosion Science and Technology Division, Indira Gandhi Centre for Atomic Research, Kalpakkam 603 102, India
E-mail: mpujar@nd.edu

S. N. MALHOTRA
Metallurgical Engineering and Materials Science, Indian Institute of Technology, Mumbai 400 076, India

T. P. S. GILL
Materials Technology Division, Indira Gandhi Centre for Atomic Research, Kalpakkam 603 102, India

Uniform or localised corrosion resistance of stainless steels is attributed to the presence of a tenacious passive film formed on the surface, the thickness and chemical composition of which depends on the applied potential. The protective properties of such films depend on the bulk composition of the alloy, presence of secondary phases and elemental segregation. In this paper the role of Cr, Mo and ferrite content on the anodic dissolution behaviour of type 316 austenitic stainless steel weld metals has been investigated. A calculational approach was tried in order to qualitatively understand the behaviour of the stainless steel weld metals with different chemical compositions and heat inputs. Extensive iterative calculations were carried out by using the experimental data on the anodic current values to arrive at the results.

1. Introduction

Dissolution behaviour of austenitic stainless steels at different cathodic and anodic potentials has been widely studied by a number of workers [1, 2]. The chemical composition of the films formed at these potentials, enrichment of alloying elements like Cr and Mo and a possible interaction between these elements have also received considerable attention. This information has been used to establish the mechanism of the corrosion resistance offered by these alloys. Several investigations were aimed at understanding the strong inhibiting effect Mo exerted on the active dissolution of the stainless steels [3–5].

Most of these studies reported, pertain to sophisticated equipments like ESCA, XPS and SAM with in-built specimen preparation and handling capability. Entire system is maintained under total inert atmosphere in order to avoid any oxidation of elements present in the film on the surface. The composition and thickness of surface films are determined by using XPS technique. Such techniques are not very successful with austenitic stainless steel weld metals which have duplex microstructure and contain microscopic inhomogeneities. The delta-ferrite present in the austenite matrix is enriched in Cr, Mo and depleted in Ni. Delta-ferrite which also exhibits active-passive dissolution characteristics [6, 7] could contribute to the formation of surface films. Interpretation of XPS data from such films could be extremely difficult due to localised changes in the elemental concentration affected by the dissolution of ferrite. In order to find out information on the dissolution behaviour of weld metals a somewhat easier and relatively more reliable method was employed. It is well known that activation overpotential. η_A is related to the dissolution current density as,

$$\eta_A = a + b \log i$$

where a and b are Tafel constants, which vary according to electrode process and solution. This suggests that rate of activation controlled electrode reaction should increase with increase in potential according to Tafel relationship [8]. Since the electrochemical reaction between the alloy and the environment takes place in the outer atomic layer, the surface composition and the surface state strongly affects corrosion parameters such as: dissolution rate, overpotential and passivability [9]. Therefore, change in the dissolution current density of different alloys at the same electrode potential values in a given environment can be correlated to the bulk chemical composition.

TABLE I Welding conditions for Stationary Arc TIG welding

Welding current	200 A
Arc gap	3 mm
Argon flow rate	6 ltr/min
Welding voltage	20 V
Welding time	75 s

2. Experimental procedure

2.1. Weld metal preparation

To prepare weld metal samples with known and controlled addition of alloying elements a novel technique was employed. This technique is known as 'Stationary Arc Tungsten Inert Gas Welding' (SATIG). With standardised welding conditions, Tungsten Inert Gas (TIG) welding was carried out at a spot on the work-piece by keeping the arc stationary for a fixed time duration, which could give required weld metal penetration. A type 316 stainless steel plate of $100 \times 100 \times 25$ mm size was used in order to dissipate the heat during welding. Welding conditions were standardised (Table I) by preparing weld metals without any alloying element addition. Ultra high purity argon gas was used for shielding the weld puddle from oxidation. Argon was used for flushing out any air present in the welding torch for 15 s prior to striking the arc. Every weld metal was prepared at the centre of the plate in order to ensure uniform cooling conditions. Addition of alloying elements during welding was accomplished by inserting the accurately weighed chips or wire pieces (of ultra high purity) of Cr and Mo by a ceramic rod to avoid any contamination. Before addition of these elements arc was struck at a lower current value (~100 A) for 5–10 s during which addition was completed. Immediately after this, welding current was raised to its standard value (~200 A) and maintained there for the desired time duration. The weld metal prepared by melting the plate for 75 s had a diameter of around 15 mm and penetration of 7–8 mm. Five weld metal specimens of this type were prepared. In order to raise the ferrite content of these weld metals accurately weighed high purity Cr chips and Mo wires were separately added during welding. Addition of 80 mg and 200 mg of Cr and 50 mg and 140 mg of Mo were carried out during making of the weld metal by melting for 75 s. Weld metals with each addition were prepared at four different heat inputs as 0.36, 0.56, 0.85 and 1.00 kJ/mm. Preparation of the weld metal is shown in Fig. 1. In order to know the chemical composition of these weld metals, number of weld metals which were melted for 75 s were prepared and drilled (up to a depth of 3 mm only) to collect weld metal chips. These were degreased and then subsequently used for wet chemical analysis.

2.2. Delta-ferrite measurement

Delta-ferrite measurement was carried out by Magnegage. This instrument was calibrated in accordance with the procedures laid out in AWS A4.2-74 [10]. For a weld metal with highest welding time of 75 s, weld metal area, being large, total of 40 readings were taken, but in case of weld metals with different heat input values, specimen area being small (~0.3 cm^2), total of 25 readings were taken, in order to arrive at an average delta-ferrite value.

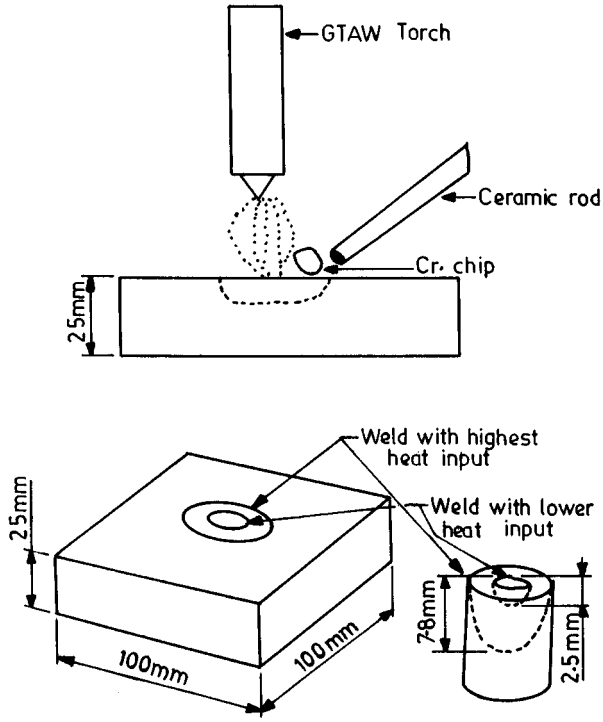

Figure 1 Representation of the stationary arc TIG (SATIG) welding by adding Cr chips (upper picture) A316 ss weld pad showing the location of the weld metal and the machined weld metal (lower picture).

2.3. Anodic polarisation experiments

The method, set-up and procedure to carry out the anodic polarisation experiment was followed as per the instructions given in the standard practice prescribed in ASTM-G5-87 standard [11]. The medium of these studies was chosen as 0.5 M H_2SO_4 containing 0.1 g/l NH_4SCN. All the solutions were purged with oxygen free argon gas for 1 h before beginning any experiment. The gas purging was continued till the completion of the experiment. Specimen to be used as a working electrode was in the form of a circular disk. All the electrode potentials were measured against Saturated Calomel Electrode (SCE). The mounted specimen was polished up to fine diamond (~1 μm) and then cleaned in soap solution, degreased and cleaned again by double distilled water before immersion. The distance between the tip of the probe and the specimen surface was maintained at 3–4 mm away from the specimen by careful positioning. Thus, the solution resistance was maintained at about 0.4 ohms and consequently the effect of IR drop was negligible for current densities smaller than 10 mA [12]. Stable Open Circuit Potential (OCP) of the specimen was measured after 1 h of its immersion. Stable OCP values were obtained in this medium. After this anodic polarisation experiment was carried out from OCP to +1000 mV(SCE) at a potential scan rate of 10 mV/min. Wenking STP 84 potentiostat was interfaced with a PC in order to be able to accurately measure the anodic current values at an interval of 1 mV

TABLE II Chemical composition of the base and weld metals with different additions of alloying elements, wt.%

Element	Base metal	Weld metal				
		Without elemental addition	80 mg Cr	200 mg Cr	50 mg Mo	140 mg Mo
Carbon	0.041	0.039	0.036	0.04	0.039	0.041
Silicon	0.60	0.61	0.60	0.59	0.60	0.57
Manganese	1.44	1.44	1.47	1.42	1.40	1.44
Sulphur	0.018	0.02	0.019	0.018	0.019	0.020
Phosphorus	0.02	0.02	0.023	0.027	0.025	0.027
Chromium	17.19	16.81	17.96	18.71	16.80	16.63
Nickel	10.76	10.61	11.07	11.39	11.07	11.23
Molybdenum	2.46	2.42	2.40	2.82	4.16	5.83

applied potential. The potential vs current density data were plotted on semilog paper to obtain polarisation diagrams.

3. Results and discussion

Chemical compositions of the weld metals along with the base metal are presented in Table II. It was noted than an addition of 80 mg and 200 mg of pure chromium chips during welding raised the weld metal chromium content from 16.81 wt.% (without elemental addition) to 17.96 wt.% (1.16 wt.% increase) and 18.71 wt.% (1.9 wt.% increase) respectively. Similarly, by addition of 50 and 140 mg of molybdenum, the initial concentration of molybdenum (2.42 wt.% without any addition) changed to 4.16 wt.% (1.74 wt.% increase) and 5.83 wt.% (3.41 wt.% increase) respectively. The carbon, nitrogen and nickel levels were found to be unchanged due to the addition of chromium and molybdenum during welding.

The specimens without any elemental addition were designated as WA. The 80 mg and 200 mg Cr added specimens were designated as Cr1 and Cr2 respectively. Similarly 50 mg and 140 mg Mo added specimens were designated as Mo1 and Mo2 respectively. The heat input values of 0.36, 0.56, 0.85, 1.00 and that due to welding for 75 s were designated as $H1$, $H2$, $H3$, $H4$ and $H5$ respectively. The designations of all specimens with different heat inputs are given in Table III. The term "Cr-added weld metals" signify WA, Cr1 and Cr2 specimens with increasing Cr contents. Similarly, the term "Mo-added weld metals" signify WA, Mo1 and Mo2 specimens with increasing Mo contents.

Delta-ferrite contents of the weld metals have been presented in Table IV. It was noted that the ferrite values of the weld metals prepared at lower heat inputs varied in a range defined by the ferrite value of the weld metal with 75 s melting time ±2FN (ferrite number). This variation in ferrite contents is not considered very significant.

TABLE III Weld metal specimen designations at different heat inputs

Heat input designation	WA	Cr1	Cr2	Mo1	Mo2
$H1$	WA$H1$	Cr1$H1$	Cr2$H1$	Mo1$H1$	Mo2$H1$
$H2$	WA$H2$	Cr1$H2$	Cr2$H2$	Mo1$H2$	Mo2$H2$
$H3$	WA$H3$	Cr1$H3$	Cr2$H3$	Mo1$H3$	Mo2$H3$
$H4$	WA$H4$	Cr1$H4$	Cr2$H4$	Mo1$H4$	Mo2$H4$
$H5$	WA$H5$	Cr1$H5$	Cr2$H5$	Mo1$H5$	Mo2$H5$

TABLE IV Delta-ferrite contents for weld metals with different chemical compositions and heat inputs

Heat input	WA	Cr1	Cr2	Mo1	Mo2
$H1$	3.4 ± 0.4	9.0 ± 0.2	14.2 ± 0.4	8.3 ± 0.2	9.6 ± 0.3
$H2$	4.0 ± 0.3	9.5 ± 0.5	10.6 ± 0.4	6.9 ± 0.2	9.2 ± 0.6
$H3$	5.0 ± 0.1	9.4 ± 0.2	10.3 ± 0.6	7.0 ± 0.3	8.9 ± 0.3
$H4$	6.5 ± 0.2	8.7 ± 0.2	9.1 ± 0.6	8.7 ± 0.5	8.7 ± 0.3
$H5$	4.2 ± 0.4	6.8 ± 0.6	12.1 ± 1.0	6.1 ± 0.5	13.3 ± 0.6

3.1. Data analysis

Current density values were tabulated at potentials spanning from −340 to −230 mV(SCE) at an interval of 10 mV (Tables V–IX). These potential values were chosen such that they were encompassed by OCP and peak potential for all samples. Data analysis was carried out for Cr-added and Mo-added weld metals separately at constant heat inputs and constant potential values. A new independent variable X was defined as,

$$X = (A1{*}\mathrm{Cr}) + (B1{*}\mathrm{FN})$$

and

$$X = (A2{*}\mathrm{Mo}) + (B2{*}\mathrm{FN})$$

TABLE V Current density values for weld metals WA in μA/cm^2 at different heat inputs

Potential (mV) (SCE)	$H1$	$H2$	$H3$	$H4$	$H5$
−230	4575	4741	3996	4262	4187
−240	3800	3863	3259	3571	3295
−250	2998	3121	2653	2876	2576
−260	2541	2629	2190	2349	2026
−270	2143	2250	1821	1822	1580
−280	1731	1925	1410	1520	1260
−290	1283	1557	1161	1263	1000
−300	976	1317	928	1041	807
−310	686	1106	735	824	657
−320	458	891	576	653	505
−330	275	664	463	478	406
−340	140	522	312	345	281

TABLE VI Current density values for weld metals Cr1 in μA/cm^2 at different heat inputs

Potential (mV) (SCE)	$H1$	$H2$	$H3$	$H4$	$H5$
−230	3587	3861	3636	5511	2851
−240	3110	3199	3034	4646	2321
−250	2698	2482	2479	3905	1856
−260	2415	2107	1890	3262	1481
−270	1936	1820	1576	2740	1189
−280	1611	1594	1337	2360	949
−290	1343	1389	1138	1880	773
−300	1038	1208	976	1576	645
−310	735	982	793	1321	548
−320	525	833	570	1099	439
−330	368	675	363	937	261
−340	269	576	237	752	143

TABLE VII Current density values for weld metals Cr2 in μA/cm^2 at different heat inputs

Potential (mV) (SCE)	$H1$	$H2$	$H3$	$H4$	$H5$
−230	4094	4137	4704	4509	4806
−240	3575	3757	4241	3945	4292
−250	2979	3241	3683	3306	3624
−260	2422	2693	3097	2725	2995
−270	1960	2188	2578	2237	2402
−280	1602	1666	2050	1865	1912
−290	1246	1373	1771	1465	1509
−300	1039	1150	1569	1233	1186
−310	867	958	1378	1028	959
−320	731	796	1174	847	766
−330	603	661	976	687	629
−340	464	568	754	560	538

TABLE VIII Current density values for weld metals Mo1 in μA/cm^2 at different heat inputs

Potential (mV) (SCE)	$H1$	$H2$	$H3$	$H4$	$H5$
−230	2656	2882	2766	3671	2099
−240	1980	2297	2079	3074	1606
−250	1579	1667	1667	2459	1229
−260	1282	1327	1329	1918	933
−270	1063	1072	1094	1384	703
−280	899	884	927	1086	483
−290	818	734	790	844	352
−300	661	659	719	637	250
−310	476	514	553	465	179
−320	306	358	373	308	108
−330	173	225	211	205	46
−340	107	119	130	129	1

where $A1$, $B1$, $A2$ and $B2$ were the constants to be determined and they are unique for a given combination of heat input and potential. In these equations ferrite was designated as "FN" for convenience. To accomplish this a data file (3 rows × 3 columns) was prepared by taking into account increasing Cr concentrations (1st column), delta-ferrite values for a given heat input (2nd column) and current density values at a given active potential (3rd column). The data analysis was carried out by iterative method so that for a unique combination of $A1$ and $B1$ (or $A2$ and $B2$), highest correlation coefficient (r) was obtained for X and the corresponding current density values, where X is defined as above. The X values which yielded highest r values were plotted against the corresponding current density values to obtain linear relationships as,

$$\text{Current density} = m1*X + C1$$

(Cr-added weld metals)

and

$$\text{Current density} = m2*X + C2$$

(Mo-added weld metals)

The actual slope values $m1$, $m2$ so obtained were used to obtain the coefficients of Cr, Mo and ferrite which affected the current density values as,

$$\text{Current density} = m1A1*\text{Cr} + m1B1*\text{FN} + C1$$

(Cr-added weld metals)

$$\text{Current density} = m2A2*\text{Mo} + m2B2*\text{FN} + C2$$

(Mo-added weld metals)

The product $m1A1$, $m1B1$, $m2A2$ and $m2B2$ were defined as the coefficients of respective elements.

The equations so obtained while determining the coefficient values for Cr and Mo added weld metals at different heat inputs are given in Tables X–XIV and Tables XV–XIX respectively. Since the magnitudes of these coefficients of Cr, Mo and ferrite decide the dissolution current, their profiles were obtained as a function of active potential (Figs 2–7). These coefficients do not have any standard units and signify the effect of Cr, Mo and ferrite on the active dissolution current at a given heat input and applied potential in arbitrary units. The Cr and Mo coefficients when obtained under constant concentration levels of other elements (like Fe, Ni etc.) signify the variation of Cr and Mo levels as a function of potential qualitatively. Positive or negative coefficients of a given element suggest either positive or negative contribution towards the anodic current density. The regions where Cr and Mo are segregated being active

TABLE IX Current density values for weld metals Mo2 in μA/cm^2 at different heat inputs

Potential (mV) (SCE)	$H1$	$H2$	$H3$	$H4$	$H5$
−230	583	686	587	448	1072
−240	506	577	526	385	867
−250	423	462	477	305	685
−260	348	376	389	211	538
−270	283	283	315	152	393
−280	213	188	255	110	315
−290	166	133	208	83	254
−300	124	96	170	66	207
−310	90	70	133	53	169
−320	64	52	107	44	150
−330	45	38	81	36	118
−340	33	19	56	27	85

TABLE X Equations obtained during data analysis of current density values to find the Cr and Ferrite coefficients at different active potentials of Cr-added weld metals for heat input = $H1$

Potential (mV) (SCE)	$X = A1*\text{Cr} + B1*\text{FN}$	C.D. $= m1*X + C1$	Cr coefficient	Ferrite coefficient
−230	$X = 6.00\text{Cr} - 1.00\text{FN}$	C.D. $= -796.40X + 82226$	−4778	796
−240	$X = 5.98\text{Cr} - 1.02\text{FN}$	C.D. $= -625.36X + 64520$	−3740	638
−250	$X = 17.01\text{Cr} - 2.98\text{FN}$	C.D. $= -111.39X + 33734$	−1895	332
−260	$X = 2.01\text{Cr} - 0.30\text{FN}$	C.D. $= -206.17X + 9299$	−414	62
−270	$X = 1.97\text{Cr} - 0.30\text{FN}$	C.D. $= -364.31X + 13841$	−718	109
−280	$X = 6.02\text{Cr} - 0.85\text{FN}$	C.D. $= -56.93X + 7329$	−343	48
−290	$X = 11.00\text{Cr} - 2.01\text{FN}$	C.D. $= 47.41X - 7164$	522	−95
−300	$X = 4.00\text{Cr} - 0.58\text{FN}$	C.D. $= 48.12X - 2149$	192	−28
−310	$X = 4.02\text{Cr} - 0.93\text{FN}$	C.D. $= -75.34X + 5542$	−303	70
−320	$X = 4.01\text{Cr} - 0.91\text{FN}$	C.D. $= -123.94X + 8434$	−497	113
−330	$X = 3.99\text{Cr} - 0.94\text{FN}$	C.D. $= -127.98X + 8454$	−511	120
−340	$X = 6.94\text{Cr} - 2.00\text{FN}$	C.D. $= -38.57X + 4381$	−268	77

TABLE XI Equations obtained during data analysis of current density values to find the Cr and Ferrite coefficients at different active potentials of Cr-added weld metals for heat input = $H2$

Potential (mV) (SCE)	$X = A1*\text{Cr} + B1*\text{FN}$	C.D. $= m1*X + C1$	Cr coefficient	Ferrite coefficient
−230	$X = 5.00\text{Cr} - 1.97\text{FN}$	C.D. $= 167.82X - 8059$	839	−331
−240	$X = 10.00\text{Cr} - 2.98\text{FN}$	C.D. $= 129.47X - 16377$	1295	−386
−250	$X = 10.98\text{Cr} - 3.02\text{FN}$	C.D. $= 151.76X - 23078$	1666	−458
−260	$X = 11.00\text{Cr} - 3.06\text{FN}$	C.D. $= 117.87X - 17743$	1297	−361
−270	$X = 10.01\text{Cr} - 2.97\text{FN}$	C.D. $= 85.00X - 11055$	851	−252
−280	$X = 2.01\text{Cr} - 0.88\text{FN}$	C.D. $= 127.04X - 1926$	255	−112
−290	$X = 1.00\text{Cr} - 1.17\text{FN}$	C.D. $= 31.30X + 1176$	31	−37
−300	$X = 4.00\text{Cr} + 0.30\text{FN}$	C.D. $= -17.46X + 2512$	−70	5
−310	$X = 3.99\text{Cr} - 4.12\text{FN}$	C.D. $= 7.15X + 743$	29	−29
−320	$X = 2.18\text{Cr} + 0.02\text{FN}$	C.D. $= -22.21X + 1707$	−48	00
−330	$X = 4.02\text{Cr} - 1.07\text{FN}$	C.D. $= -7.80X + 1159$	−31	8
−340	$X = 4.01\text{Cr} - 1.93\text{FN}$	C.D. $= -8.64X + 1039$	−35	17

TABLE XII Equations obtained during data analysis of current density values to find the Cr and Ferrite coefficients at different active potentials of Cr-added weld metals for heat input = $H3$

Potential (mV) (SCE)	$X = A1*\text{Cr} + B1*\text{FN}$	C.D. $= m1*X + C1$	Cr coefficient	Ferrite coefficient
−230	$X = 10.01\text{Cr} - 3.03\text{FN}$	C.D. $= 223.32X - 30179$	2235	−677
−240	$X = 6.97\text{Cr} - 2.00\text{FN}$	C.D. $= 352.30X - 34474$	2456	−705
−250	$X = 6.98\text{Cr} - 1.97\text{FN}$	C.D. $= 347.88X - 34717$	2428	−685
−260	$X = 9.98\text{Cr} - 2.93\text{FN}$	C.D. $= 249.48X - 35986$	2490	−731
−270	$X = 7.00\text{Cr} - 2.05\text{FN}$	C.D. $= 293.72X - 29713$	2056	−602
−280	$X = 10.99\text{Cr} - 3.05\text{FN}$	C.D. $= 129.75X - 20569$	1426	−396
−290	$X = 11.00\text{Cr} - 2.97\text{FN}$	C.D. $= 113.60X - 18147$	1250	−337
−300	$X = 3.99\text{Cr} - 1.02\text{FN}$	C.D. $= 284.97X - 16723$	1137	−291
−310	$X = 3.98\text{Cr} - 1.01\text{FN}$	C.D. $= 282.38X - 16722$	1124	−285
−320	$X = 15.00\text{Cr} - 4.00\text{FN}$	C.D. $= 78.88X - 17727$	1183	−316
−330	$X = 7.00\text{Cr} - 1.99\text{FN}$	C.D. $= 177.15X - 18609$	1240	−353
−340	$X = 6.98\text{Cr} - 1.97\text{FN}$	C.D. $= 149.40X - 15737$	1043	−294

from −440 to −400 mV(SCE) did not contribute to the formation of these profiles.

In general, the profiles of Cr coefficients (Fig. 2) showed a trend where the values either remained constant or increased with increase in potential and towards the end, they decreased rapidly. This decrease was found to be steepest at $H1$. This is in concurrence with the fact that Cr dissolved more than Mo due to its less noble OCP. In fact, among Fe, Cr, Mo and Ni, Cr is known to have most active corrosion potential (E_{corr}) in 0.5 M H_2SO_4 medium [9]. But with increase in potential, the enrichment of Mo on the metal/solution interface leads to some sort of interatomic forces that decrease the overall dissolution rate of the alloy [9]. The decrease in Cr coefficients towards the end could be attributed to this phenomenon.

It is reported [13] that the stainless steel specimens (21.7Cr-17.3Ni-3.6Mo) when polarised in chloride solution at various active potentials (from −300 to −100 mV(SCE)) showed a continuous increase in the Cr cations found in the oxide films formed on the surface and quantitatively detected by ESCA. This observation has been confirmed by other workers [9, 14]. An interesting observation could be made from

TABLE XIII Equations obtained during data analysis of current density values to find the Cr and Ferrite coefficients at different active potentials of Cr-added weld metals for heat input = $H4$

Potential (mV) (SCE)	$X = A1{*}\text{Cr} + B1{*}\text{FN}$	C.D. $= m1{*}X + C1$	Cr coefficient	Ferrite coefficient
−230	$X = 1.00\text{Cr} - 0.77\text{FN}$	C.D. $= -2300.90X + 31420$	−2301	1772
−240	$X = 1.00\text{Cr} - 0.82\text{FN}$	C.D. $= -1655.13X + 22569$	−1655	1357
−250	$X = 0.99\text{Cr} - 0.84\text{FN}$	C.D. $= -1449.84X + 19084$	−1435	1218
−260	$X = 1.00\text{Cr} - 0.84\text{FN}$	C.D. $= -1302.33X + 17135$	−1302	1094
−270	$X = 1.00\text{Cr} - 0.86\text{FN}$	C.D. $= -1241.00X + 15743$	−1241	1067
−280	$X = 1.00\text{Cr} - 0.84\text{FN}$	C.D. $= -1198.50X + 15126$	−1199	1007
−290	$X = 1.00\text{Cr} - 0.81\text{FN}$	C.D. $= -976.10X + 12530$	−976	791
−300	$X = 1.00\text{Cr} - 0.82\text{FN}$	C.D. $= -822.11X + 10480$	−822	674
−310	$X = 1.00\text{Cr} - 0.84\text{FN}$	C.D. $= -709.23X + 8876$	−709	596
−320	$X = 1.00\text{Cr} - 0.85\text{FN}$	C.D. $= -618.41X + 7630$	−618	526
−330	$X = 1.00\text{Cr} - 0.86\text{FN}$	C.D. $= -620.02X + 7434$	−620	533
−340	$X = 1.00\text{Cr} - 0.90\text{FN}$	C.D. $= -489.63X + 5711$	−490	441

TABLE XIV Equations obtained during data analysis of current density values to find the Cr and Ferrite coefficients at different active potentials of Cr-added weld metals for heat input = $H5$

Potential (mV) (SCE)	$X = A1{*}\text{Cr} + B1{*}\text{FN}$	C.D. $= m1{*}X + C1$	Cr coefficient	Ferrite coefficient
−230	$X = 3.99\text{Cr} - 1.06\text{FN}$	C.D. $= -743.16X + 50762$	−2965	788
−240	$X = 3.01\text{Cr} - 0.87\text{FN}$	C.D. $= -834.98X + 42533$	−2513	726
−250	$X = 3.00\text{Cr} - 0.91\text{FN}$	C.D. $= -685.67X + 34567$	−2057	624
−260	$X = 3.01\text{Cr} - 0.94\text{FN}$	C.D. $= -552.93X + 27849$	−1664	520
−270	$X = 2.99\text{Cr} - 0.96\text{FN}$	C.D. $= -425.44X + 21267$	−1272	408
−280	$X = 3.00\text{Cr} - 0.96\text{FN}$	C.D. $= -337.65X + 16944$	−1013	324
−290	$X = 3.00\text{Cr} - 0.97\text{FN}$	C.D. $= -253.91X + 12782$	−762	246
−300	$X = 3.01\text{Cr} - 0.98\text{FN}$	C.D. $= -183.55X + 9348$	−552	180
−310	$X = 2.99\text{Cr} - 1.00\text{FN}$	C.D. $= -133.77X + 6825$	−400	134
−320	$X = 2.99\text{Cr} - 1.05\text{FN}$	C.D. $= -98.16X + 5011$	−294	103
−330	$X = 3.00\text{Cr} - 0.92\text{FN}$	C.D. $= -139.76X + 6919$	−419	129
−340	$X = 2.99\text{Cr} - 0.94\text{FN}$	C.D. $= -143.59X + 6939$	−429	135

TABLE XV Equations obtained during data analysis of current density values to find the Mo and Ferrite coefficients at different active potentials of Mo-added weld metals for heat input = $H1$

Potential (mV) (SCE)	$X = A2{*}\text{Mo} + B2{*}\text{FN}$	C.D. $= m2{*}X + C2$	Mo coefficient	Ferrite coefficient
−230	$X = 20.08\text{Mo} - 1.04\text{FN}$	C.D. $= -64.41X + 7480$	−1293	67
−240	$X = 20.92\text{Mo} + 2.00\text{FN}$	C.D. $= -39.28X + 6053$	−822	−79
−250	$X = 10.97\text{Mo} + 0.99\text{FN}$	C.D. $= -59.04X + 4761$	−648	−58
−260	$X = 19.09\text{Mo} + 2.97\text{FN}$	C.D. $= -26.22X + 4014$	−501	−78
−270	$X = 17.05\text{Mo} + 3.00\text{FN}$	C.D. $= -24.20X + 3385$	−413	−73
−280	$X = 12.01\text{Mo} + 1.01\text{FN}$	C.D. $= -32.12X + 2774$	−386	−32
−290	$X = 22.00\text{Mo} - 2.00\text{FN}$	C.D. $= -19.82X + 2139$	−436	59
−300	$X = 11.03\text{Mo} - 1.99\text{FN}$	C.D. $= -33.82X + 1653$	−373	67
−310	$X = 5.01\text{Mo} - 0.97\text{FN}$	C.D. $= -54.11X + 1166$	−271	52
−320	$X = 6.03\text{Mo} - 0.99\text{FN}$	C.D. $= -27.44X + 768$	−165	27
−330	$X = 9.00\text{Mo} - 0.95\text{FN}$	C.D. $= -9.31X + 448$	−84	9
−340	$X = 9.00\text{Mo} - 2.03\text{FN}$	C.D. $= -5.94X + 229$	−54	12

the profiles of ferrite (Fig. 3) obtained along with those of Cr in Cr-added weld metals.

The coefficients of Cr and those of ferrite always complemented each other at all the potentials. The coefficients of ferrite were found to be sharply increasing at those heat inputs where corresponding Cr coefficients sharply decreased. This could be attributed to the dissolution and subsequent passivation of ferrite. The dissolution current density was simultaneously dependent on Cr and ferrite coefficients in the active potential range.

There are definite evidences in literature [13, 15, 16] where it has been shown that during dissolution of stainless steels in active range of potentials, iron is selectively dissolved and the alloying elements are enriched on the surface in their metallic state. It is known that Ni is not oxidised due to the fact that its oxidation power is low compared to the oxidation of Cr, Fe and Mo which been confirmed by ESCA studies on the stainless steels [9]. In the present work, it was contended that the Cr and Mo coefficients could be considered to be factors that suggested the equivalent amount of enrichment of the respective metal/metal oxide on the surface of the weld metal/solution interface in the polarised condition. It has been observed by Brox and Olefjord [9] that

TABLE XVI Equations obtained during data analysis of current density values to find the Mo and Ferrite coefficients at different active potentials of Mo-added weld metals for heat input = $H2$

Potential (mV) (SCE)	$X = A2{*}\text{Mo} + B2{*}\text{FN}$	C.D. $= m2{*}X + C2$	Mo coefficient	Ferrite coefficient
−230	$X = 13.98\text{Mo} - 5.03\text{FN}$	C.D. $= -190.61X + 7401$	−2665	959
−240	$X = 7.05\text{Mo} - 2.02\text{FN}$	C.D. $= -244.52X + 6084$	−1724	494
−250	$X = 1.00\text{Mo} + 3.99\text{FN}$	C.D. $= -109.15X + 5105$	−109	−436
−260	$X = 2.94\text{Mo} - 5.12\text{FN}$	C.D. $= 133.68X + 4381$	393	−684
−270	$X = 4.01\text{Mo} - 4.95\text{FN}$	C.D. $= 159.82X + 3825$	641	−791
−280	$X = 3.98\text{Mo} - 4.91\text{FN}$	C.D. $= 142.19X + 3312$	566	−698
−290	$X = 1.00\text{Mo} - 1.72\text{FN}$	C.D. $= 253.46X + 2665$	253	−436
−300	$X = 2.09\text{Mo} + 3.07\text{FN}$	C.D. $= -52.50X + 2219$	−110	−161
−310	$X = 1.02\text{Mo} - 2.16\text{FN}$	C.D. $= 131.63X + 1903$	134	−284
−320	$X = 1.00\text{Mo} - 0.98\text{FN}$	C.D. $= 482.73X + 1590$	483	−473
−330	$X = 1.00\text{Mo} - 0.83\text{FN}$	C.D. $= 658.98X + 1232$	659	−545
−340	$X = 1.00\text{Mo} - 0.76\text{FN}$	C.D. $= 864.61X + 1024$	865	−657

TABLE XVII Equations obtained during data analysis of current density values to find the Mo and Ferrite coefficients at different active potentials of Mo-added weld metals for heat input = $H3$

Potential (mV) (SCE)	$X = A2{*}\text{Mo} + B2{*}\text{FN}$	C.D. $= m2{*}X + C2$	Mo coefficient	Ferrite coefficient
−230	$X = 1.00\text{Mo} - 0.91\text{FN}$	C.D. $= 56479.60X + 125952$	56480	−51396
−240	$X = 1.00\text{Mo} - 0.92\text{FN}$	C.D. $= 27212.50X + 63364$	27213	−25036
−250	$X = 1.00\text{Mo} - 0.93\text{FN}$	C.D. $= 15507.80X + 37680$	15508	−14422
−260	$X = 1.00\text{Mo} - 0.97\text{FN}$	C.D. $= 6211.20X + 17473$	6211	−6025
−270	$X = 1.00\text{Mo} - 0.98\text{FN}$	C.D. $= 4563.78X + 13277$	4564	−4473
−280	$X = 1.00\text{Mo} - 0.92\text{FN}$	C.D. $= 11520.60X + 26862$	11521	−10599
−290	$X = 1.00\text{Mo} - 0.91\text{FN}$	C.D. $= 15687.50X + 35023$	15688	−14276
−300	$X = 1.00\text{Mo} - 0.90\text{FN}$	C.D. $= 26487.10X + 56714$	26487	−23838
−310	$X = 1.01\text{Mo} - 0.91\text{FN}$	C.D. $= 14806.20X + 32258$	14954	−13474
−320	$X = 1.00\text{Mo} - 0.92\text{FN}$	C.D. $= -4676.08X + 10904$	4676	−4302
−330	$X = 8.00\text{Mo} - 7.03\text{FN}$	C.D. $= -908.63X - 14074$	−7269	6388
−340	$X = 8.00\text{Mo} - 7.06\text{FN}$	C.D. $= -824.07X - 12997$	−6593	5818

TABLE XVIII Equations obtained during data analysis of current density values to find the Mo and Ferrite coefficients at different active potentials of Mo-added weld metals for heat input = $H4$

Potential (mV) (SCE)	$X = A2{*}\text{Mo} + B2{*}\text{FN}$	C.D. $= m2{*}X + C2$	Mo coefficient	Ferrite coefficient
−230	$X = 3.01\text{Mo} - 1.94\text{FN}$	C.D. $= -637.89X + 863$	−1920	1238
−240	$X = 3.00\text{Mo} - 1.93\text{FN}$	C.D. $= -534.04X + 748$	−1602	1031
−250	$X = 3.00\text{Mo} - 1.91\text{FN}$	C.D. $= -428.03X + 669$	−1284	818
−260	$X = 4.99\text{Mo} - 2.96\text{FN}$	C.D. $= -204.20X + 887$	−1019	604
−270	$X = 2.00\text{Mo} - 1.03\text{FN}$	C.D. $= -367.05X + 1140$	−734	378
−280	$X = 8.99\text{Mo} - 4.03\text{FN}$	C.D. $= -64.81X + 1232$	−583	261
−290	$X = 11.03\text{Mo} - 4.06\text{FN}$	C.D. $= -41.22X + 1276$	−455	167
−300	$X = 3.98\text{Mo} - 1.00\text{FN}$	C.D. $= -85.86X + 1310$	−342	86
−310	$X = 7.98\text{Mo} - 1.03\text{FN}$	C.D. $= -30.91X + 1214$	−247	32
−320	$X = 4.98\text{Mo} + 1.00\text{FN}$	C.D. $= -31.76X + 1243$	−158	−32
−330	$X = 7.00\text{Mo} + 2.98\text{FN}$	C.D. $= -14.53X + 1006$	−102	−43
−340	$X = 4.99\text{Mo} + 4.03\text{FN}$	C.D. $= -12.26X + 814$	−61	−49

chemical gradients existed in the neighbourhood of the surface during dissolution suggesting thereby that solid state diffusion had taken place during formation of the outer metal/metal oxide.

The Mo coefficients for Mo added weld metals have been presented in Figs 4 and 5. The coefficients owing to their very high values at all potentials observed at $H3$ were separately plotted in Fig. 5. The profiles were almost similar to those observed for Cr coefficients, except at $H3$, where, the Mo coefficients continuously increased towards the more noble potentials. The gradual decrease in the Mo coefficients observed in Fig. 4 could be compared with the profile of Mo cation found in the oxide film formed at various active potentials [13] in stainless steel (21.7Cr-17.3Ni-3.6Mo). Mo cation content actually decreased continuously in the active potential range of −300 to −100 mV(SCE). It is reported that the dissolution coefficients of Cr (Z_{cr}) and Mo (Z_{Mo}) change synchronically at any applied potential. The corresponding ferrite coefficients have been presented in Figs 6 and 7.

Olefjord [15] reported the results of his investigation by ESCA on Fe-18Cr-3Mo, Fe-17Cr-13Ni and Fe-17Cr-13Ni-2.6Mo alloys which were polarised at

TABLE XIX Equations obtained during data analysis of current density values to find the Mo and Ferrite coefficients at different active potentials of Mo-added weld metals for heat input = $H5$

Potential (mV) (SCE)	$X = A2{*}\text{Mo} + B2{*}\text{FN}$	C.D. $= m2{*}X + C2$	Mo coefficient	Ferrite coefficient
−230	$X = 4.99\text{Mo} - 1.28\text{FN}$	C.D. $= -339.67X + 6483$	−1695	435
−240	$X = 10.99\text{Mo} - 3.04\text{FN}$	C.D. $= -128.89X + 5097$	−1417	392
−250	$X = 7.00\text{Mo} - 2.03\text{FN}$	C.D. $= -165.20X + 3984$	−1156	335
−260	$X = 10.00\text{Mo} - 3.03\text{FN}$	C.D. $= -95.86X + 3140$	−959	290
−270	$X = 13.00\text{Mo} - 3.97\text{FN}$	C.D. $= -59.34X + 2469$	−771	236
−280	$X = 4.00\text{Mo} - 1.39\text{FN}$	C.D. $= -184.53X + 1981$	−738	257
−290	$X = 11.00\text{Mo} - 4.02\text{FN}$	C.D. $= -58.04X + 1577$	−638	233
−300	$X = 7.99\text{Mo} - 3.07\text{FN}$	C.D. $= -71.32X + 1278$	−570	219
−310	$X = 5.01\text{Mo} - 1.99\text{FN}$	C.D. $= -99.91X + 1043$	−501	199
−320	$X = 7.01\text{Mo} - 2.98\text{FN}$	C.D. $= -63.14X + 796$	−443	188
−330	$X = 8.99\text{Mo} - 3.99\text{FN}$	C.D. $= -46.46X + 647$	−418	185
−340	$X = 13.01\text{Mo} - 6.01\text{FN}$	C.D. $= -26.10X + 452$	−340	157

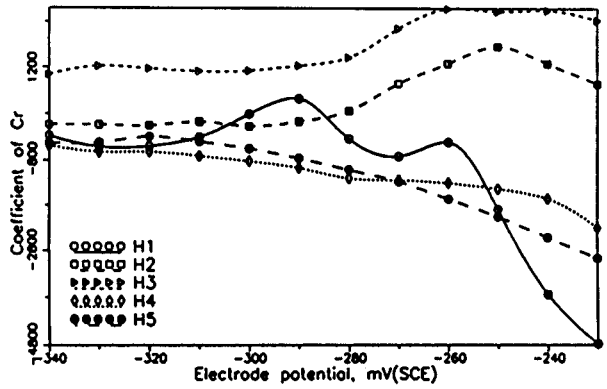

Figure 2 Profiles of coefficients of Cr as a function of potentials during active dissolution of the weld metal.

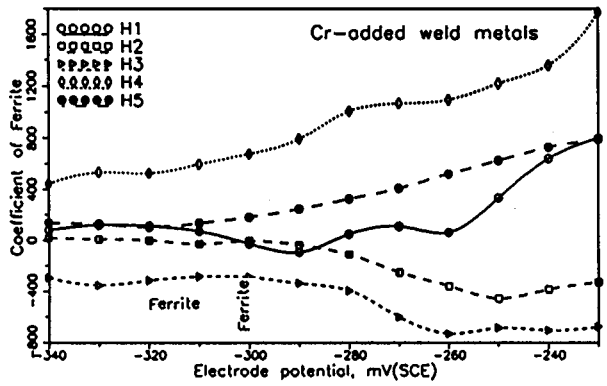

Figure 3 Profiles of coefficients of Ferrite as a function of potentials during active dissolution of the weld metal.

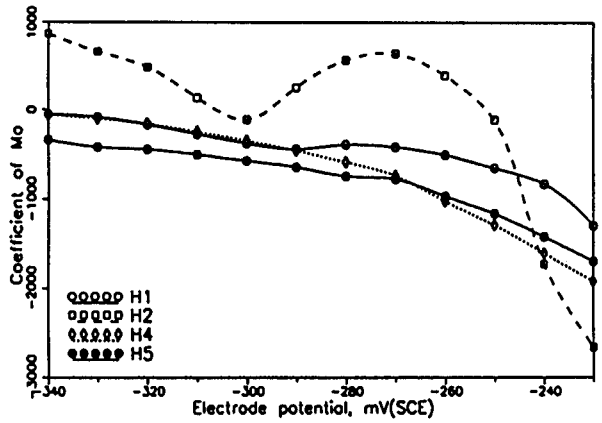

Figure 4 Profiles of coefficients of Mo as a function of potentials during active dissolution of the weld metal.

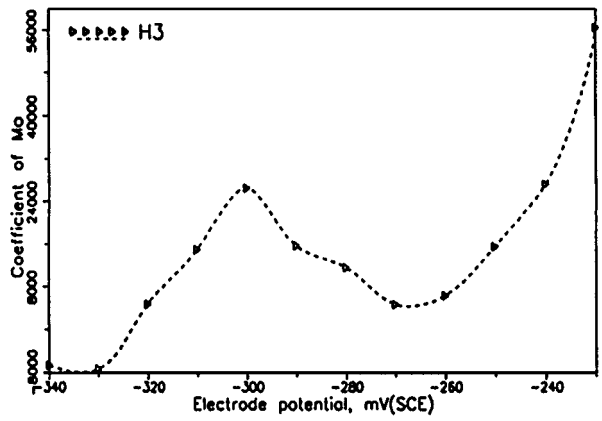

Figure 5 Profiles of coefficients of Mo as a function of potentials during active dissolution of the weld metal.

different cathodic, anodic and passive potentials in 0.1 M HCl + 0.1 M NaCl solution. He observed that only after polarising in the active potential range, he could observe high Mo content in the film which was again correlated with the selective dissolution of Fe. Olefjord *et al*. [15] reported that the selective dissolution of Fe was controlled by the interatomic forces over the interface (metal/solution and between the alloying elements). This kind of selective dissolution reportedly led to the formation of intermetallic compounds like σ, χ and laves phases which generally form at high temperatures, due to the interaction between atoms. It has been documented that [15] for three alloys *viz*. Fe-18Cr, Fe-28Cr and Fe-18Cr-3Mo, irrespective of the applied potential, the enrichment was largest for the Mo alloyed steel. He attributed this observation to the synergistic interaction between Mo and Cr which had a direct bearing on the dissolution. The Cr and Mo coefficients were plotted at different heat inputs at constant potentials (Figs 8 and 9). The profiles of Cr coefficients (Fig. 8) were found to be increasing gradually up to $H3$ and thereafter decreased to a low value and remained invariant till the highest heat input, $H5$. The profiles of Mo coefficients (Fig. 9), in general showed a maxima at $H3$ at all the potentials but remained invariant on either low or high heat inputs. The Mo coefficients were found

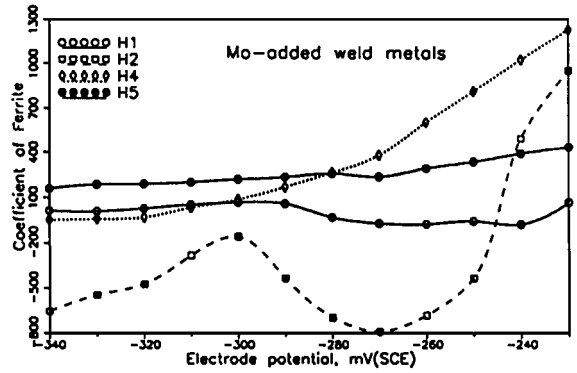

Figure 6 Profiles of coefficients of Ferrite as a function of potentials during active dissolution of the weld metal.

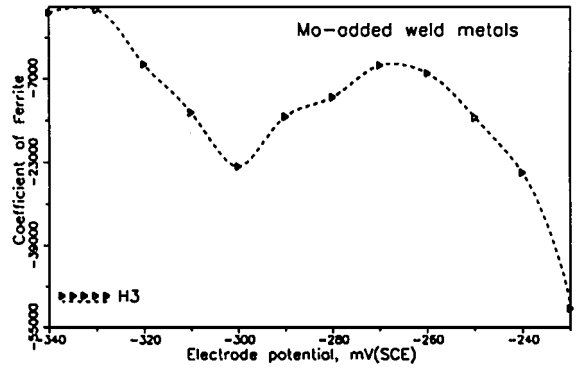

Figure 7 Profiles of coefficients of Ferrite as a function of potentials during active dissolution of the weld metal.

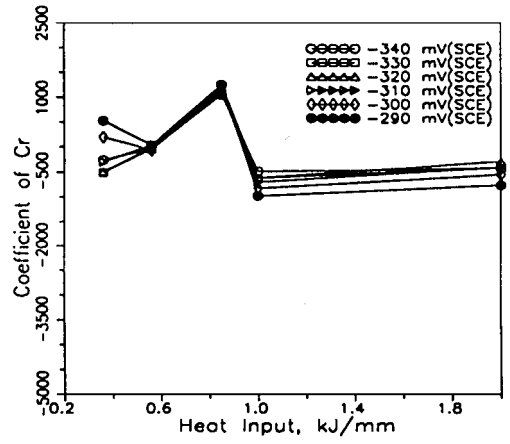

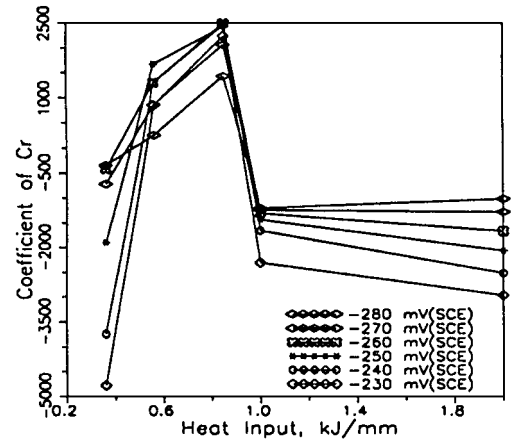

Figure 8 Coefficients of Cr as a function of heat input at different potentials.

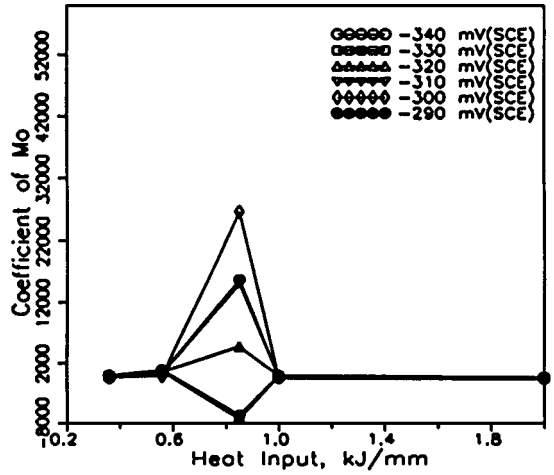

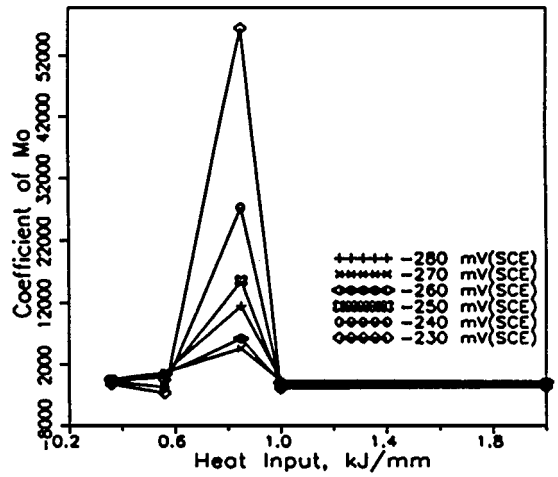

Figure 9 Coefficients of Mo as a function of heat input at different potentials.

to be higher at every potential as well as at every heat input as compared to the Cr coefficients. The Mo coefficients at $H3$ were several orders of magnitude higher as compared to the corresponding Cr coefficients. In the light of these observations it could be suggested that the synergistic interaction between Mo and Cr played a major role in decreasing the active dissolution. The enrichment of Mo and Ni is attributed to the fact that they are more noble than Fe and Cr. The interatomic forces between Mo and Cr slow down the dissolution rate of Cr and thereby it also gets enriched on the surface. Thereafter a steady state is reached when overall dissolution rate is lowered [5].

The implication of this result could be realised from the peak current density as well as peak potential values (see Table XX). The drastic reduction in the peak current density values for 5.83 wt.% Mo added weld metals is clearly noticeable. In a similar fashion shift in the primary passivation potentials (E_{pp}) in the active direction is also significant for Mo added weld metals as compared to Cr added weld metals.

3.2. Role of ferrite during active dissolution

Anodic polarisation curves of delta-ferrite and sigma (Fig. 10) show that the Flade potential of sigma phase is much more active as compared to that of the delta-ferrite

TABLE XX Peak potential (P, in mV(SCE)) and peak current density values (c.d. in μA/cm^2) of the weld metals

	WA		Cr1		Cr2		Mo1		Mo2	
Heat input	p	c.d.	p	c.d.	p	c.d.	p	c.d.	p	c.d.
$H1$	−194	6506	−199	4567	−218	4506	−201	3598	−218	629
$H2$	−195	6893	−195	5321	−213	4274	−197	4115	−217	750
$H3$	−189	6075	−198	4688	−219	4900	−200	3747	−224	596
$H4$	−188	7124	−197	7127	−219	4993	−210	4267	−218	478
$H5$	−185	7257	−187	4438	−211	5108	−195	3029	−207	1371

in acidified ammonium thiocyanate medium [7]. If consequent to the enrichment of alloying elements like Cr, Mo and Ni, intermetallic phases like sigma formed [13] during active dissolution, the surface would be completely passivated at the Flade potential of sigma leaving the ferrite network still actively dissolving.

This kind of behaviour of ferrite was supported by the coefficients of ferrite which were found to be increasing at the end of the active potentials at all heat inputs. Subsequently ferrite dissolution started decreasing (the difference between its peak potential and Flade potential is sufficiently large, Fig. 10) and contributed towards reduction in the overall peak current density. The correlation between coefficients of Cr and Mo and their corresponding ferrite coefficients at each potential significantly supported this concept (Figs 11–13).

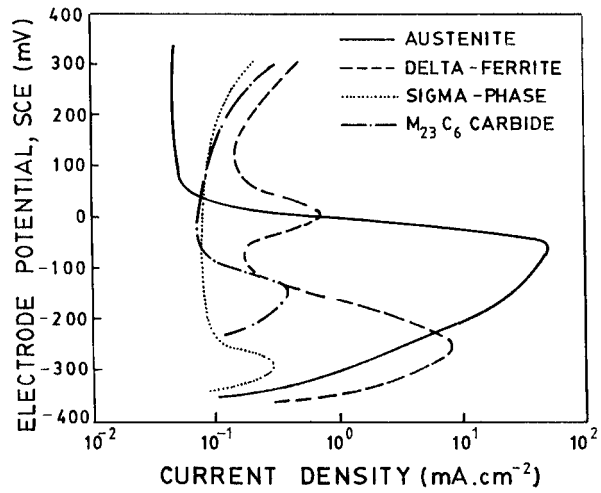

Figure 10 Anodic polarisation diagrams of pure delta-ferrite and pure sigma in 3.6N H_2SO_4 + 0.01N NH_4SCN [9].

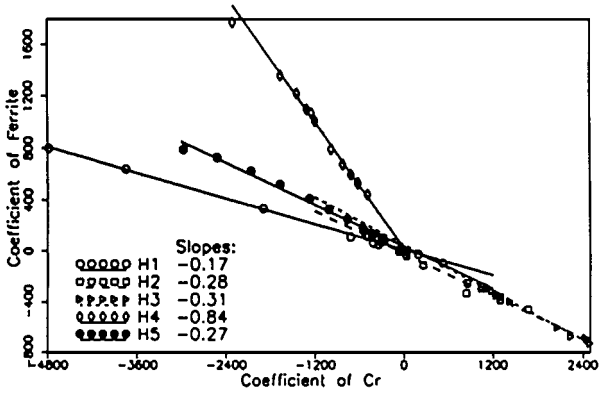

Figure 11 Relation between coefficients of Cr and Ferrite (from −340 to −230 mV(SCE)) at constant heat inputs for Cr added weld metals.

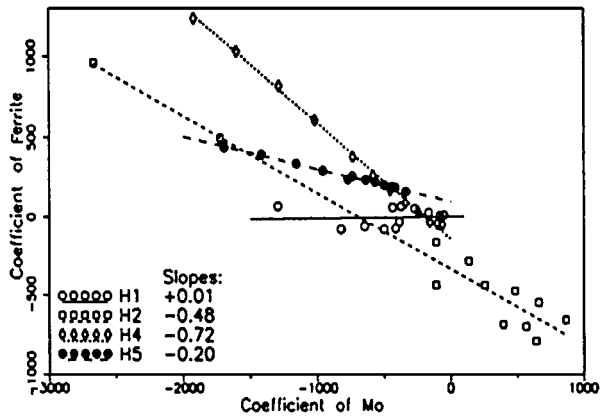

Figure 12 Relation between coefficients of Mo and Ferrite (from −340 to −230 mv(SCE)) at constant heat inputs for Mo added weld metals.

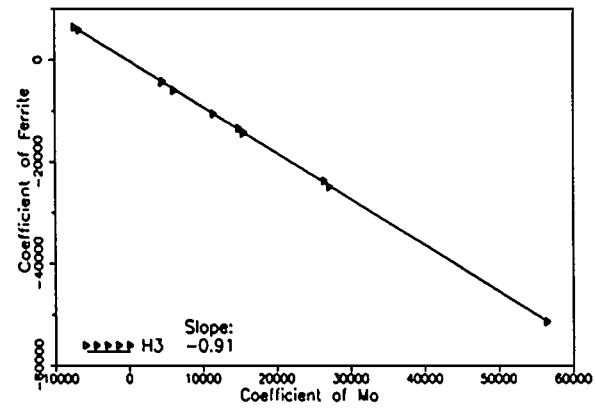

Figure 13 Relation between coefficients of Mo and Ferrite (from −340 to −230 mV(SCE)) at constant heat input for Mo added weld metals.

It was noted that all the plots were linear in nature with negative and decreasing slopes except for the weld metals at $H5$. It was found that in the range of heat inputs ($H1$ to $H4$) the contribution of Cr and Mo coefficients increased steadily with increasing potential in the noble direction which could be attributed to the enrichment of these elements with more anodic potentials. Towards the end such an enrichment and possible formation of some kind of intermetallic compounds (σ, χ, laves phase) followed by its passivation and subsequent dissolution and passivation of ferrite helped in synergistically passivating the weld metal.

4. Role of Cr and Mo during active dissolution

Alloys containing more than 12% Cr are passive down to much more negative potentials than pure Fe which is closely related to the properties of pure Cr [17]. There

have been many investigations [18–20] related to the studies on the electrochemical behaviour of Fe-Cr alloys elucidating the role of Cr at different applied potentials. Anodic polarisation behaviour of Fe-Cr alloys depends upon the Cr content of the alloy and it has been contended [21] that up to 17% Cr addition led to the formation of two anodic peaks similar to that of pure Fe and the behaviour was altered only when Cr content was raised to beyond 22%. At this concentration of Cr the alloy behaved like pure Cr. In the present investigation although the Cr content varied between 16.8 to 18.7%, due to the addition of other alloying elements like Mo and Ni, a single anodic peak was observed for all weld metals. Alexandre *et al*. [19] carried out anodic polarisation experiments on Fe-Cr alloys containing 10 to 22% Cr by using rotating disc electrode in molar sulphuric acid and arrived at the relationship for measured current, $I(\Omega)$ as function of rotation speed (Ω) as,

$$I(\Omega) = A + \mathrm{Id}(\Omega)$$

where A represented the non-diffusional component (independent of Ω) and Id was the diffusional component of the total current. Though Id was found to be small fraction of A, it was observed that Id increased with increasing Cr content as well as potential during active dissolution. The authors contended that increase in the potential raised the relative weightage of the diffusional path as the Cr content increased. These factors led to the transfer of alloying elements towards the surface leading to the enrichment. Dissolution of Mo containing alloys is affected by dissolution behaviour of pure Mo metal in the electrolyte under consideration. Pure Mo shows active-passive behaviour only in alkaline medium [21]. Its dissolution behaviour in aggressive media like acidic chlorides (HCl + NaCl solutions) led to its spontaneous passivation which was followed by its transpassive dissolution [9, 13, 15, 22, 23]. It is reported that pure Mo directly started to dissolve above -0.03 V(SCE) in both 1N HCl as well as in 1N H_2SO_4 solutions [24]. In general, it was found that the OCP of Mo in all the media was always more noble when compared with pure Fe, Cr and Ni. Although there were number of different views on the role of Mo during active dissolution, still it was unanimously agreed from the results of a large number of ESCA analyses that, Mo exerted a strong inhibiting effect on active dissolution [4, 25–28]. Asami *et al*. [1] reported that the faster the dissolution of Mo containing alloys, higher was the content of the Mo in the corrosion deposits which suppressed the active dissolution. This Mo which got enriched on the surface inhibited the dissolution by way of limiting the diffusion rate by replacing Fe and Cr at the oxide/metal interface [26]. Its noble OCP and subsequent inert (it exists in partially elemental and partially in MoO_2 oxide from [2]) behaviour in most of the acidic media led to the active dissolution of Fe and Cr while it got enriched in the elemental form at the surface below which hydrated Cr and Fe oxyhydroxide film grew [29]. The slower dissolution of Mo in turn reduced the overall dissolution of the alloy [30]. The inhibiting effect of the Mo was found useful only in active potential range because as the anodic potential was raised beyond E_{pp}, the Mo suffered from the transpassive dissolution [22] which could again be prevented from increasing the Cr content of the alloy. This implies that, stainless steels containing Cr and Mo acted in a synergistic way in resisting the corrosion attack as reported earlier [1, 15, 22, 31]. Extensive XPS studies on Cr-Ni-Mo alloys (in 12 M HCl) were carried out to prove that such an effect actualy came into force to increase the corrosion resistance [32]. It is imperative that the alloy contained certain minimum amount of Cr along with Mo, in order for the synergistic effect to come into force [24]. It is reported that a minimum of 2% Mo is required in order to be effective in arresting active dissolution of the alloy [33]. Based on these views Olefjord [14] suggested that electrochemical dissolution rate constant depends on both the Cr and Mo contents at the metal surface. This could be expressed as,

$$\upsilon_M = k_M * C_M$$

and

$$k_M = \nu \exp(-\Delta G^\circ / RT) \exp\{f(\beta, V)\}$$

where υ_M is the dissolution rate of the species M and k_M is the electrochemical rate constant, C_M is the concentration, ν is the lattice vibration frequency, ΔG° is the standard free energy for activation of atomic jumps from the lattice to a point in the Helmholtz double layer and β and V are symmetry factor and the potential respectively. It was suggested [15] that the ΔG° values of Mo and Cr synergistically increased for the Cr-Mo alloyed steels which lowered the dissolution rates of these elements. Physically this means that the bonding of the surface atoms is enhanced by the simultaneous enrichment of Cr and Mo. The "Surface phase" is formed due to enrichment of these elements which has a greater thermodynamic stability than that of the solid solution. This explains the synergistic effect that helps increase the corrosion resistance of Cr, Mo alloys.

5. Conclusions

Role of Cr, Mo and ferrite on the active dissolution were studied in this paper. Active potentials from -340 to -230 mV(SCE) which were encompassed between OCP and E_{pp} were chosen for these studies. Effect of added Cr and Mo would be reflected on the change in the active dissolution current density, concentration of remaining alloying elements being constant. Following conclusions were drawn from the above investigations:

1. Data analysis carried out by using iterative method resulted in yielding what is termed as the "Cr coefficients" and "Mo coefficients". These were qualitatively considered to be equivalent to the amounts of these elements enriched on the polarised metal surface at that potential. This was based on the fundamental Tafel relation.
2. To a large extent, the profiles of the coefficients of Cr and Mo when plotted against the applied potential

were found to be similar to those plots experimentally obtained by earlier workers by using surface sensitive techniques.

3. It was found that Mo played a significant role in inhibiting the dissolution of the alloy in the active potential range by getting enriched on the alloy/electrolyte interface. Enrichment of Mo in either elemental or in MoO_2 form on the surface and its subsequent slow dissolution allowed the formation and growth of the Cr and Fe hydrate oxyhydroxide film beneath it. This led to the suppresson of the active dissolution of the alloy. Beyond E_{pp}, the dissolution was controlled by the pesence of Cr as the Mo started to dissolve in its transpassive region. A definite synergism existed between the added Cr and Mo that inhibited the active dissolution of the alloy.

4. The enrichment of Cr, Mo and Ni on the polarised surface allowed the formation of some sort of phase which was similar to that of sigma in chemical composition. Since sigma passivated before the passivation of ferrite, ferrite continued to dissolve and contributed to dissolution current density. Thereafter ferrite slowly passivated. Therefore the role of ferrite could be termed as complementary to that of Cr and Mo during active dissolution.

Acknowledgements

The authors wish to thank Dr. H. S. Khatak, Head, Corrosion Science & Technology Division, Dr. V. S. Raghunathan, Associate Group Director, Materials Characterisation Group (MCG) and Dr. Baldev Raj, Director, Metallurgy and Materials Group (MMG), IGCAR, Kalpakkam for their keen interest and support during the course of the above investigation.

References

1. K. ASAMI, M. NAKA, K. HASHIMOTO and T. MASUMOTO, *J. Electrochem. Soc*. **127** (1980) 2130.
2. B. BROX and I. OLEFJORD, "Stainless Steels '84" (The Institute of Metals, London, 1985) p. 134.
3. I. OLEFJORD and B.-O. ELFSTROM, *Corrosion* **38** (1982) 46.
4. R. C. NEWMAN, *Corr. Sci*. **25** (1985) 331.
5. K. HASHIMOTO, K. ASAMI and K. TERAMOTO, *ibid*. **19** (1979) 3.
6. R. GOETZ and D. LANDOLT, *Electrochim. Acta* **27** (1982) 1061.
7. S. JIN and A. ATRENS, *Appl. Phys*. **A46** (1988) 51.
8. T. G. GOOCH, The Welding Institute Research Bulletin 1974, p. 183.
9. T. P. S. GILL and J. B. GNANAMOORTHY, *J. Mater. Sc*. **17** (1982) 1513.
10. L. L. SHREIR, R. A. JARMAN and G. T. BURSTEIN, "CORROSION-Metal/Environment Reaction," 3rd ed. Vol. 1 (Butterworth-Heinsmanss Ltd., Oxford, 1994) pp. 1–88, 1–106.
11. AWS A 2-74: Standard procedures for calibrating magnetic instruments to measure the delta-ferrite content of austenitic stainless steel weld metal.
12. ASTM-G5-87: "Annual Book of ASTM Standards," Section 3, Vol. 03.02, (ASTM, Philadelphia, 1992) pp. 73–79.
13. Y. H. YAU and M. A. STREICHER, *Corrosion* **47** (1991) 352.
14. I. OLEFJORD, *Mater. Sci. & Engg*. **42** (1980) 161.
15. I. OLEFJORD and B. BROX, "Passivity of Metals and Semiconductors," edited by M. Froment (Elsevier Science Publishers, Amsterdam, 1983) p. 561
16. I. OLEFJORD, B. BROX and U. JELVESTRAM, *J. Electrochem. Soc*. **132** (1985) 2854.
17. S. HAUPT and H. H. STREHBLOW, *Corr. Sci*. **37** (1995) 43.
18. I. EPELBOIN, M. KEDDAM, O. R. MATTOS and H. TAKENOUTI, *ibid*. **19** (1979) 1105.
19. B. ALEXANDRE, A. CAPRANI, J. C. CHARBONNIER, M. KEDDAM and P. H. MOREL, *ibid*. **21** (1981) 765.
20. R. OLIVER, Thesis, Leiden, 1955.
21. M. KLIMMECK, Z. METALLKUNDE, **70** (1979) 260.
22. P. Y. PARK, E. AKIYAMA, A. KAWASHIMA, K. ASAMI and K. HASHIMOTO, *Corr. Sci*. **37** (1995) 1843.
23. Y. C. LU and C. R. CLAYTON, *ibid*. **29** (1989) 927.
24. K. SUGIMOTO and Y. SAWADA, *ibid*. **17** (1977) 425.
25. H. C. BROOKES, J. W. BAYLES and F. J. GRAHAM, *J. Appl. Electrochem*. **20** (1990) 223.
26. C. A. OLSSON, *Corr. Sci*. **37** (1995) 467.
27. J. N. WANKLYN, *ibid*. **21** (1981) 211.
28. P. MARCUS and J. OUDAR, *Appl. Suf. Sci*. **3** (1979) 48.
29. K. HASHIMOTO, "Passivity of Metals and Semiconductors," edited by M. Froment (Elsevier, Amsterdam, 1983) p. 247.
30. F. J. GRAHAM, H. C. BROOKES and J. W. BAYLES, *J. Appl. Electrochem*. **20** (1990) 45.
31. M. A. STREICHER, *Corrosion* **30** (1974) 77.
32. P. Y. PARK, E. AKIYAMA, H. HABAZAKI, A. KAWASHIMA, K. ASAMI and K. HASHIMOTO, *Corr. Sci*. **36** (1994) 1395.
33. M. A. A. TULLMIN and F. P. A. ROBINSON, *Corrosion* **44** (1988) 664.

Received 5 August 1997
and accepted 20 July 1999